JOURNAL OF MOLECULAR SPECTROSCOPY 166, 423–440 (1994)

Ab Initio Investigation of the Structure of the $X\,^2A'$, $A\,^2A''$ ($1\,^2\Pi$) Spectral System of HCO: Investigation of the Magnetic Hyperfine Effects

M. STAIKOVA, M. PERIĆ,[1] B. ENGELS, AND S. D. PEYERIMHOFF

Institut für Physikalische und Theoretische Chemie, Universität Bonn, Wegelerstrasse 12, D-53115 Bonn, Germany

Results of an ab initio study of the hyperfine structure of the $X\,^2A'$, $A\,^2A''$ ($1\,^2\Pi$) system of the formyl radical are presented. Special attention is paid to the analysis of the interplay between the vibronic and magnetic hyperfine effects. The results of computations are in very good agreement with the available experimental findings. The values for the hyperfine coupling constants in lower bending levels of both electronic species are predicted. © 1994 Academic Press, Inc.

1. INTRODUCTION

This paper represents the second part of an ab initio study devoted to elucidation of the structure of the $X\,^2A'$, $A\,^2A''$ ($1\,^2\Pi$) spectral system of HCO and DCO. In the first paper (*1*) the results of computations of the bending level energies, the moments for the transitions between vibronic states, and the spin–orbit splitting of the vibronic levels are presented. In the present paper we report the results of calculations of the hyperfine coupling constants (hfcc's). The vibronic mean values of the hfcc's are computed combining the data for electronical mean values of these quantities with the potential surfaces obtained in our previous studies (*1–4*).

Hyperfine structure of the ground electronic state of HCO and DCO has been the subject of numerous experimental studies (*5–18*). On the other hand, the theoretical information is rather scarce (*19–22*). To our knowledge there have been no publications concerning the hyperfine effects in the $A\,^2A''$ state so far. Thus we hope that the results of the present study, which is focused primarily on the analysis of the interplay between the vibronic and magnetic hyperfine couplings, will contribute to an understanding of the hyperfine structure of the spectra considered and could be of use in future experimental investigations.

2. TECHNICAL DETAILS

The most computer time consuming part of the present study concerns the calculation of the electronic mean values of the isotropic hfcc and the Cartesian components of the anisotropic hf tensor in both states considered. The isotropic hfcc, A_{iso}, is the proportionality factor between the scalar product of the nuclear spin vector operator **I** with the electron spin operator **S** and the corresponding part of the Hamiltonian (see, for example, Ref. (*8*)); it is defined for a nucleus N as

[1] Permanent address: University of Belgrade, Faculty of Science, Institute of Physical Chemistry, Studentski trg 16, P.O. Box 550, 11001 Belgrade, Yugoslavia.

0022-2852/94 $6.00
Copyright © 1994 by Academic Press, Inc.
All rights of reproduction in any form reserved.

$$A_{iso}^{N} = \frac{8}{3}\pi g_N g \beta_N \beta_e \frac{1}{S}\langle \Psi | \sum_k \delta(r_{kN}) s_{ak} | \Psi \rangle, \quad (1)$$

where β_N and g_N are the nuclear magneton and nuclear g factor, respectively. The term g is the g value for the electrons in the free radical (assumed to be 2.0) and β_e is the Bohr magneton. The sum on the right-hand side of Eq. (1) runs over all electrons; $\delta(r_{kN})s_{ak}$ indicates that only the spin density at the position of the nucleus considered is taken into account. The subscript a in the term s_{ak} indicates that the z axis is chosen to coincide with the principal moment of intertia axis a at the linear nuclear arrangement. The $x(\equiv C)$ axis is assumed to be perpendicular to the molecular plane. Ψ represents generally the total molecular wavefunctions; in the computation of the electronic mean values for the hfcc's ("electronic hfcc's") it is replaced by the electronic wavefunctions of the state in question, calculated in the framework of the Born-Oppenheimer approximation.

The anisotropic part of the hf operator for the nucleus N is represented by a traceless tensor with Cartesian components with respect to a molecule-fixed frame given by

$$A_{ij}^{N} = g_N g \beta_N \beta_e \frac{1}{S}\langle \Psi | \left(\sum_k \frac{3_{ij} - r^2 \delta_{ij}}{r^5} \right)_{k_N} s_{ak} | \Psi \rangle, \quad (2)$$

with $i, j = a, b, c$. In the present study only the diagonal matrix elements with respect to the electronic states are computed; the off-diagonal elements $\langle {}^2A' | A_{xy} | {}^2A'' \rangle$ and $\langle {}^2A' | A_{xz} | {}^2A'' \rangle$ are neglected because they do not contribute significantly to the vibronical mean values of the hfcc's ("vibronic hfcc's").

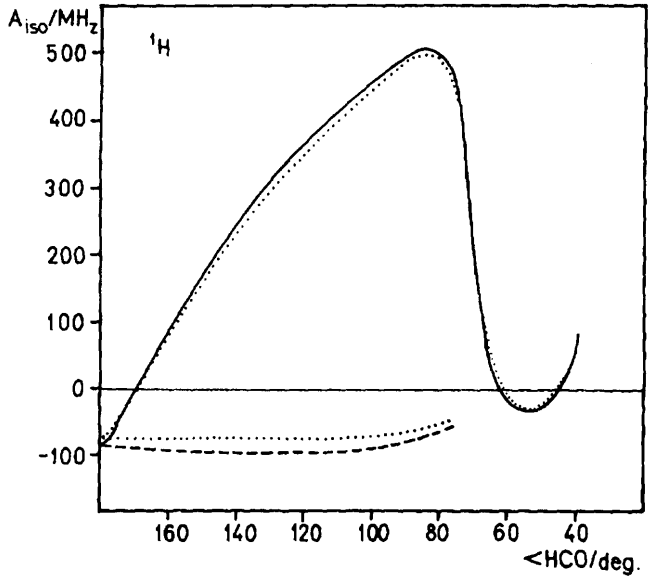

FIG. 1. Valence-bond angle dependence of the isotropic hfcc for ^{1}H in the $X\,^2A'$ (full line) and the $A\,^2A''$ (dashed line) electronic states of HCO, computed employing the MRD-CI method accompanied by a B_K correction of the electronic wavefunctions (full lines). Dotted lines represent the results of computations in which the B_K correction is not carried out. In the calculations the H–C and C–O bond lengths are kept fixed at the values of 2.0980 and 2.213153 Bohr, respectively.

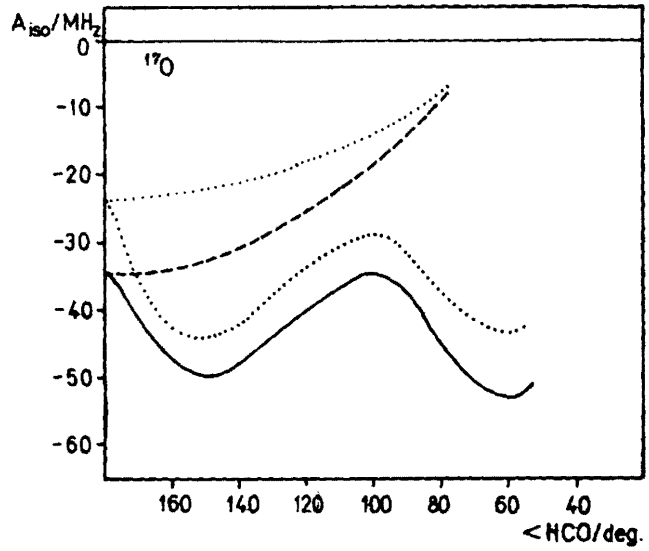

FIG. 2. Computed bond angle dependence of the isotropic hfcc for ^{17}O in the X^2A' and A^2A'' states of HCO. See the legend to Fig. 1 for notation.

Three AO basis sets are tested for the computation of the electronic hfcc's: (i) the basis proposed by Chipman (*23*) augmented by two *d* functions given by Dunning (*24*) centered on the carbon and oxygen atoms ($\alpha^C_{1d} = 1.120$, $\alpha^C_{2d} = 0.2800$, $\alpha^O_{1d} = 2.200$, $\alpha^O_{2d} = 0.550$); (ii) the same basis augmented by very compact *s* functions, in the following called "cusp functions," centered at C and O ($\alpha^C = 21\,163.05$, $\alpha^O = 39\,082.7$) and two cusp functions on the hydrogen center ($\alpha^H_1 = 639.75$, $\alpha^H_2 = 319.875$); (iii) a larger basis ($13s8p3d$) → [$9s5p3d$]. The (*sp*) basis was given by van Duijneveldt

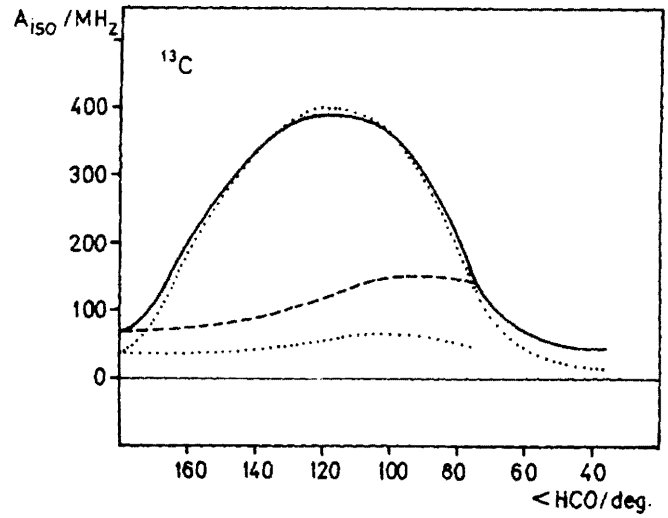

FIG. 3. Bond angle dependence of the isotropic hfcc for ^{13}C. See the legend to Fig. 1 for notation.

(*25*), and the *d* functions are taken from previous calculations of hfcc's. Test computations have shown that the larger basis gave similar results as basis (i). The influence of the cusp functions has been found to improve substantially the description of the isotropic hfcc's, particularly for the hydrogen atom. Thus all the computations presented in Section 3 are carried out employing basis (ii).

All computations of the electronic hfcc's, also at the linear molecular geometry, are carried out in terms of the C_s point group. The electronic wavefunctions are calculated by means of the multireference Single and Double excitation Configuration Interaction (MRD-CI) method (*26*) in connection with a modified B_K correction (*27*). In these calculations all electrons are correlated and no virtual orbitals are discarded. Approximate natural orbitals (NOs) for both electronic states in question are used as the one-electron basis. The number of reference configurations in the MRD-CI procedure is between 15 and 20, leading to a sum of their squared coefficients in the final CI wavefunction of about 0.92. The dimension of the MRD-CI space generated by single and double excitations with respect to these reference species is around 10^7. The threshold of $T = 2$ μhartree is the chosen criterion for configuration selection and the

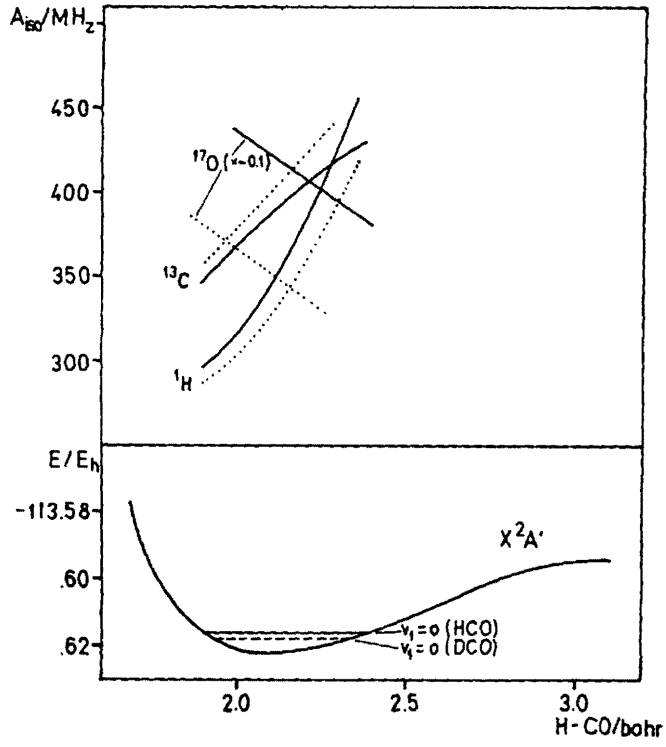

FIG. 4. (Bottom) H–CO stretching potential curve for the X^2A' state of HCO computed with the C–O bond length kept fixed at 2.221 Bohr and the bond angle value at 125°. The position of the lowest-lying vibrational level in HCO and DCO is indicated. (Top) Dependence of the values for the isotropic hfcc's in the X^2A' electronic state of HCO computed with the C–O bond length and the bond angle kept fixed at the values of 2.221 Bohr and 125°, respectively. Full lines are B_K values, and dotted lines are MRD-CI results (without B_K correction). Note that the function for ^{17}O presented in the figure has to be multiplied by the factor −0.1 (see also Fig. 2).

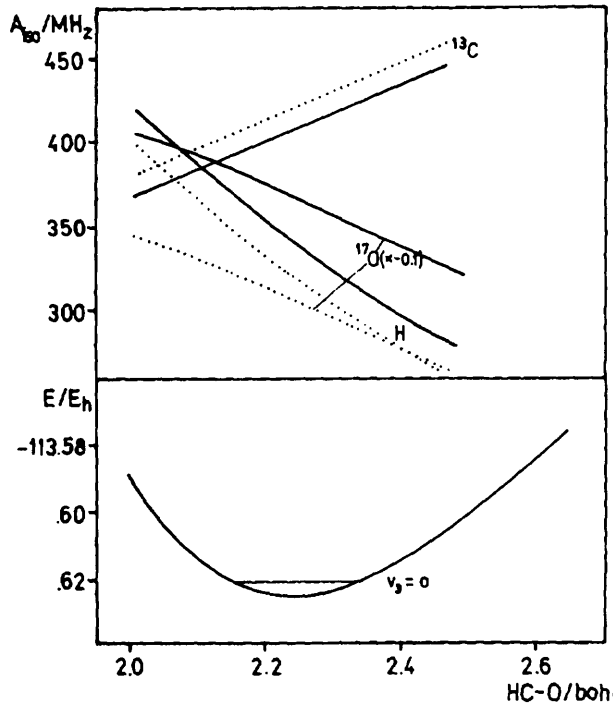

FIG. 5. (Bottom) HC–O stretching potential curve for the X^2A' state of HCO computed at the H–C bond length kept fixed at the value of 2.127 Bohr and the bond angle value of 125°. (Top) HC–O bond length dependence of the isotropic hfcc's. See the legend to Fig. 4 for notation.

truncated MRD-CI wavefunctions involve 20 000–25 000 symmetry-adapted functions (SAFs). In the framework of the B_K treatment, all coefficients in the CI expansion with the magnitude greater than 0.03 (between 500 and 700) as well as those belonging to the single excitations with respect to the leading reference configuration are corrected.

Electronic hfcc's are computed for the bond angle values of 180°, 160°, 140°, 125°, 120°, 100°, 80°, 60°, and 30° at H–C and C–O bond lengths kept fixed at 2.098 and 2.21315 Bohr, respectively. In order to estimate the influence of the stretching vibrations on the hfcc's, at the bond angle value of 125° the electronic hfcc's are calculated along the one-dimensional H–CO and HC–O sections.

Vibronically averaged hfcc's are obtained according to the approach described elsewhere (*28–30*). In these computations the vibronic wavefunctions calculated in the first part of our ab initio study of the X^2A', A^2A'' ($1^2\Pi$) system (*1*) are employed. In the present paper we publish the results for vibronical mean values of the isotropic hfcc constants for the lowest vibronical level. The values for vibronically averaged elements of the anisotropic hf tensor are also given.

3. RESULTS

Computed bond angle dependence of the electronic hfcc's for ^{1}H, ^{13}C, and ^{17}O in the X^2A' and A^2A'' states of HCO is displayed in Figs. 1–3. The pictures contain the results obtained with the truncated MRD-CI wavefunctions (dotted lines) and those

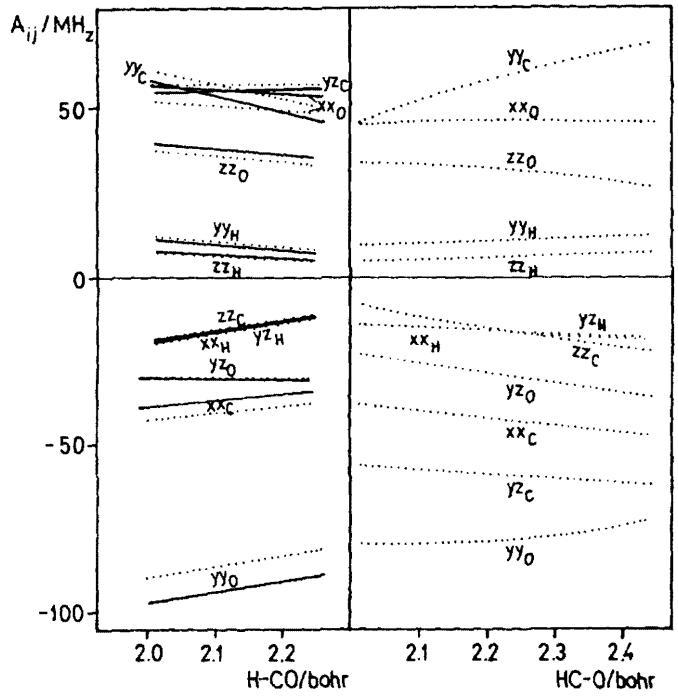

FIG. 6. (Left) H–C bond length dependence of the Cartesian components of the anisotropic hf tensor for ^1H, ^{13}C, and ^{17}O in the X^2A state of HCO computed with the C–O bond length kept fixed at 2.221 Bohr and the bond angle value at 125°. Dotted lines are results of the MRD-CI calculations, and full lines are B_K corrected values. The x axis of the coordinate system is assumed to be perpendicular to the molecular plane; the z axis is along the C–O bond. (Right) The C–O bond length dependence of the components of the hf anisotropic tensor computed on the MRD-CI level of sophistication with the H–C bond length kept fixed at 2.127 Bohr and the bond angle value at 125°.

calculated with the electronic wavefunctions corrected by means of the B_K approach (full lines). As has been stated in a number of previous studies on similar systems, an improvement of the truncated CI function is of great importance for reliable computations of the hfcc's, particularly of the isotropic coupling constants (*27*). In the case of the hydrogen atom (Fig. 1), the absolute values for the isotropic hfcc in both electronic states computed with the help of the B_K corrected wavefunctions are rather uniformly higher (by 10–20 MHz in the wide range of the bond angle variations) than the values obtained with the truncated MRD-CI wavefunctions. The situation is qualitatively similar for ^{17}O where the absolute values for A_{iso} obtained with the wavefunction are 5–10 MHz larger (15–20%) than their uncorrected CI counterparts (Fig. 2). The effect of the B_K correction is much more dramatic in the case of the carbon atom. The B_K values in the A^2A'' state are roughly twice as large as their CI counterparts. In the electronic ground state X^2A' for $\measuredangle HCO > 140°$ and $\measuredangle HCO < 100°$ the B_K corrected values are larger than the uncorrected values. Around the minimum $\measuredangle HCO = 125°$ the opposite trend is found.

The effect of the B_K correction on the values for A_{iso} of ^1H and ^{13}C becomes continuously more pronounced by the elongation of the H–C bond length—see Fig. 4, which contains the values for the X^2A' state at the bond angle value of 120°; the

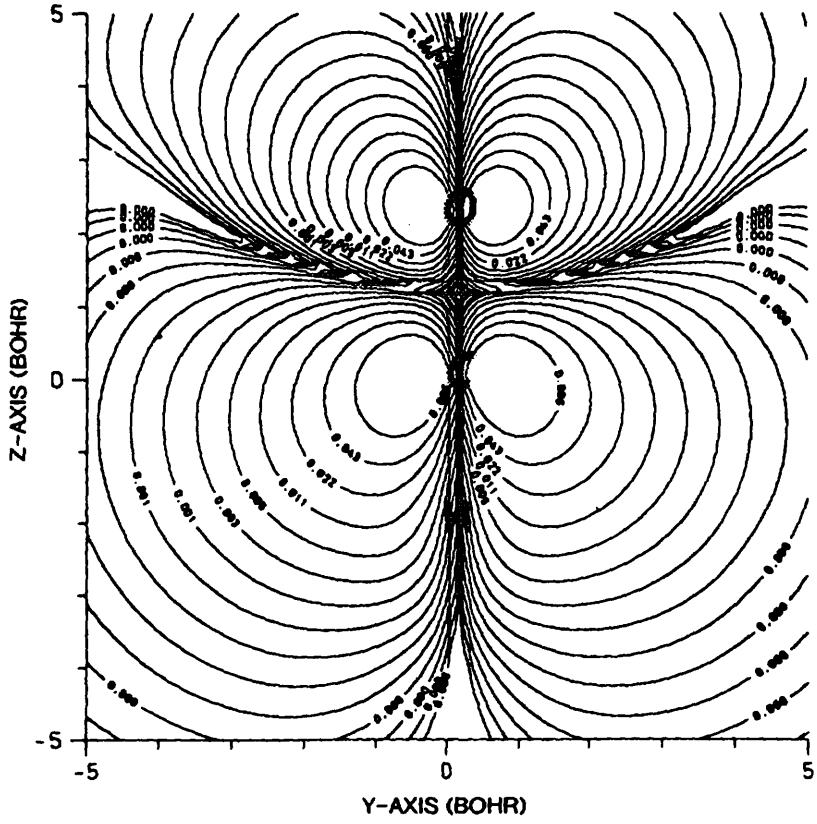

FIG. 7. Charge density contours of the singly occupied orbital (SOMO) $7a'$ of the X^2A' ground state for the linear geometry. A cut through the molecular plane is given; the positions of the nuclei are indicated.

absolute value of the A_{iso} for ^{17}O computed at the B_K level is 5–8 MHz (i.e., roughly 10–20%) larger than the corresponding CI result in the whole range of the H–C bond length variation considered (1.927–2.327 Bohr). The situation for the C–O bond length variation is presented in Fig. 5.

In accordance with the experience with other related species, the values for the components of the anisotropic hf tensor are found to be less sensitive with respect to the computational method than those of the isotropic hfcc's. Particularly, the B_K correction is less important. As an illustration Fig. 6 contains the H–C bond length dependence of the components of the anisotropic hf tensor in the electronic ground state. The bond angle HCO and the C–O bond length are kept fixed at their approximate equilibrium values. The B_K and CI curves (practically straight lines in all instances) have qualitatively the same shape; the maximal discrepancies in the corresponding results do not exceed 10%. The C–O bond length dependence of the anisotropic hf tensor is given on the right side of Fig. 6.

The isotropic hfcc's for the X^2A' state show a much more pronounced dependence on the bond angle value than their A^2A'' counterparts (Figs. 1–3). This is a consequence of the shape of the orbitals singly occupied in the various states. For the excited state A'' the singly occupied orbitals (π_x^* orbital of the CO bond) possess a node within the

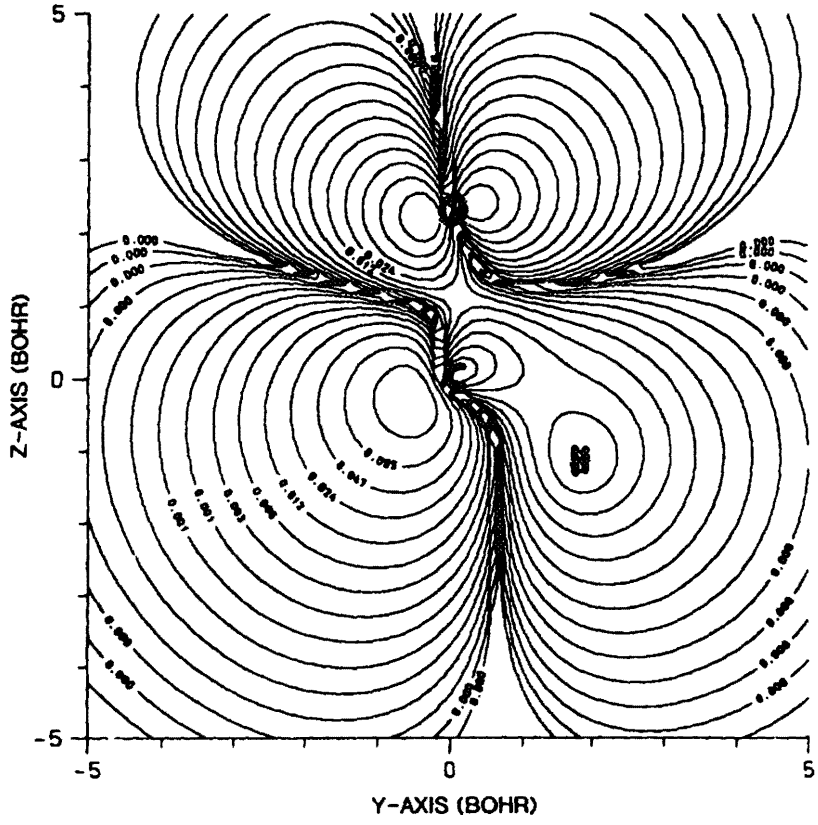

FIG. 8. Charge density contours of the SOMO $7a'$ of the X^2A' ground state for the equilibrium geometry ($\measuredangle$HCO = 125°). A cut through the molecular plane is given; the positions of the nuclei are indicated.

molecular plane. Therefore for all bond angle values the isotropic hfcc is solely determined by spin polarization effects. As a result, small absolute values are found for all geometries. The situation is the same as for the $^2B_1$ state of the NH_2 molecule (*28*).

For the X^2A' electronic ground state particularly large changes are found for A_{iso} (^{1}H), which increase from −88 to 335 MHz if the bond angle is decreased from 180° to 125° (equilibrium angle), and A_{iso} (^{13}C), which for the same bond angle variation changes from 66 to 385 MHz. The maximum of A_{iso} (^{1}H) is obtained for $\measuredangle$HCO around 90°. For smaller angles a sharp decrease of A_{iso} (^{1}H) exists. A_{iso} (^{1}H) becomes negative for $\measuredangle$HCO around 50°, but increases again for $\measuredangle$HCO < 40°. A similar behavior is found for A_{iso} (^{13}C), while A_{iso} (^{17}O) depends considerably less on the bonding angle.

The strong effects found in the electronic ground state can be explained by the shape of the singly occupied orbital $7a'$, which for different bond angles (180°, 125°, 50°) is displayed in Figs. 7–9. For $\measuredangle$HCO equal to 180° (Fig. 7) the $7a'$ represents the π_y^* CO orbital. Because the density of the orbital is zero at the position of all nuclei the isotropic hfcc are determined by spin polarization effects only with the

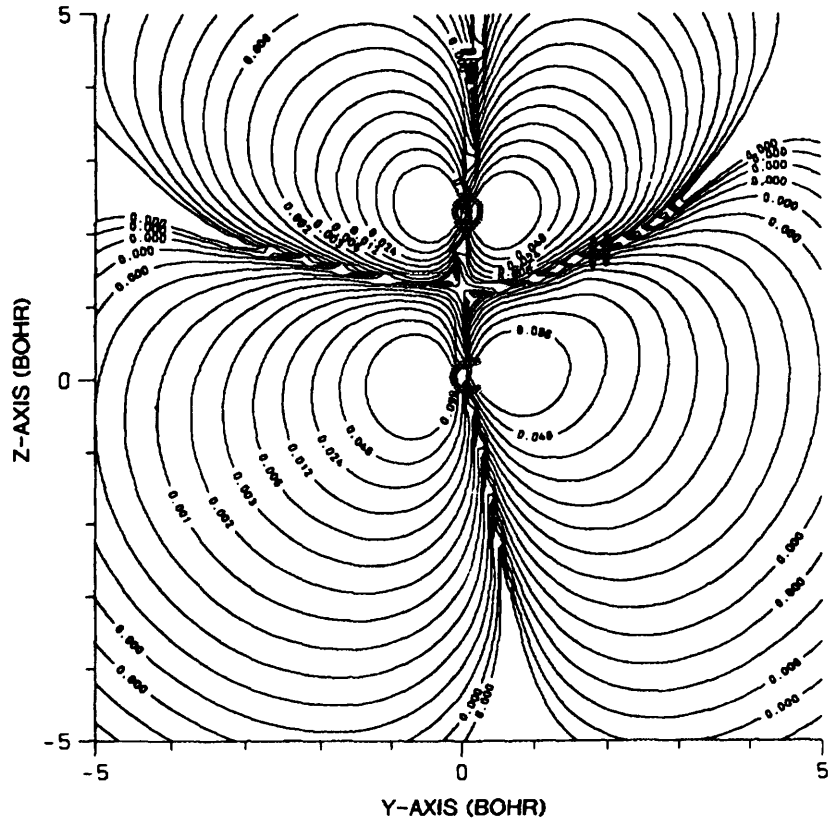

FIG. 9. Charge density contours of the SOMO $7a'$ of the X^2A' ground state for very small bond angles ($\measuredangle$HCO = 50°). A cut through the molecular plane is given; the positions of the nuclei are indicated.

consequence that small absolute values are found for all centers. For bond angles smaller than 180° in addition to the π^*_{CO} type the orbital possesses σ bond character between the carbon and the hydrogen center (Fig. 8). As a consequence the density of the $7a'$ orbital at the position of the hydrogen and carbon center is unequal to zero. Because the orbital is singly occupied large positive contributions to A_{iso} (^{1}H) and A_{iso} (^{13}C) result. For A_{iso} (^{1}H) these positive contributions overcompensate the negative spin polarization effects and A_{iso} (^{1}H) becomes positive for $\measuredangle$HCO larger than 170°. Since around the oxygen center the π^* character of the orbital is mainly retained, only small changes are found for A_{iso} (^{17}O).

The situation changes for $\measuredangle$HCO smaller than 90°. The hydrogen center moves into the region of the nodal plane which, due to the π^*_{CO} character of the orbital, separates the carbon and the oxygen center (Fig. 9) from one another. As a consequence the density of the $7a'$ orbital at the hydrogen becomes smaller and A_{iso} (^{1}H) decreases sharply. Its value drops below zero, because as for $\measuredangle$HCO = 180° spin polarization effects become very important. For $\measuredangle$HCO smaller than 50° bonding effects between the oxygen and the hydrogen are found. As a consequence A_{iso} (^{1}H) increases again.

While the dependence of the magnitude of the isotropic hfcc's on the C–O bond length in the X^2A' state is nearly linear for all three centers (Fig. 5), the H–C depen-

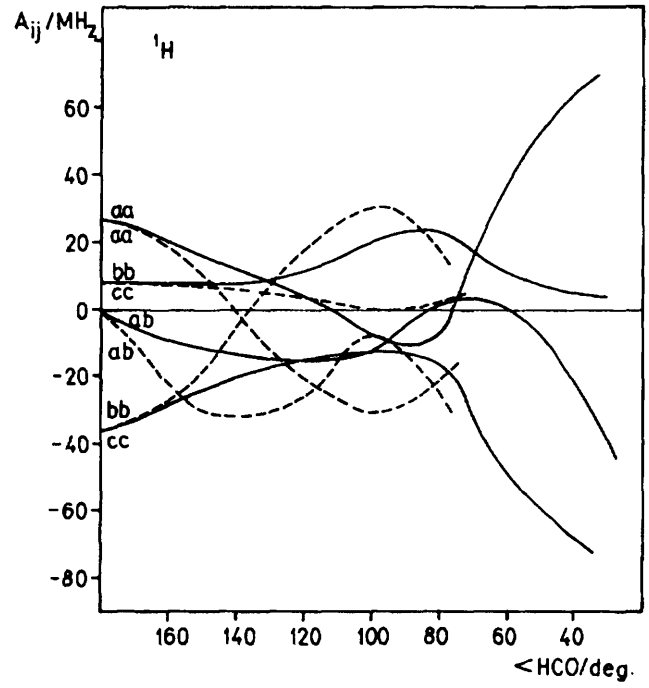

FIG. 10. Bond angle dependence of the components of the anisotropic hf tensor for the hydrogen atom in the X^2A' (full lines) and A^2A'' (dashed lines) states of HCO. The a axis is assumed to coincide with the C–O bond; the c axis is perpendicular to the molecular plane. In the computations the H–C and C–O bond lengths are kept fixed at the values of 2.127 and 2.221 Bohr, respectively.

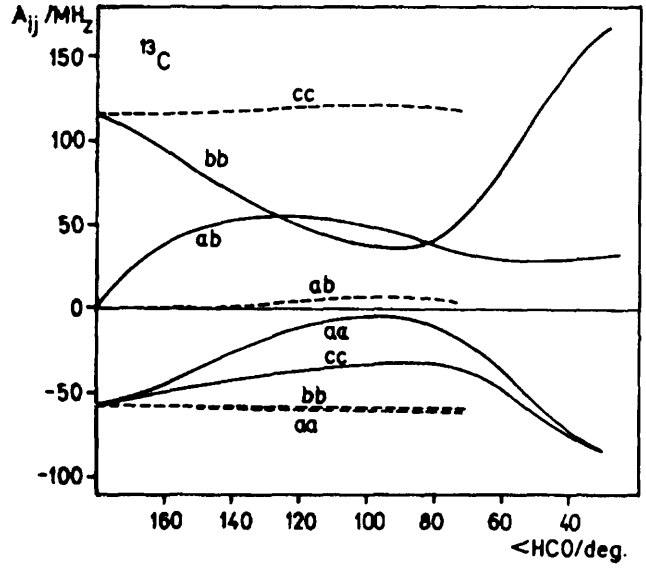

FIG. 11. Angular dependence of the anisotropic hfcc's of ^{13}C. See legend to Fig. 10 for notation.

dence for ^1H is significantly nonlinear (Fig. 4). Consequences of this behavior will be discussed below.

The bond angle dependences of the Cartesian components of the anisotropic hf tensor for both electronic states in question are displayed in Figs. 10–12. They are related to the coordinate system in which the z axis lies along the C–O bond and the x axis is perpendicular to the molecular plane. The hydrogen atom is assumed to lie in the second quadrant ($z < 0$, $y > 0$) of the yz plane.

In order to facilitate the comparison with the corresponding experimental results the Cartesian components of the dipolar hf tensor in the three coordinate systems mostly used by the experimentalists (*9*) are presented in Figs. 13–15. This includes: (i) the principal axis system of the electron spin g tensor in which the z axis is assumed to be parallel to the C–O bond; (ii) the principal moment of inertia axis system (for $^1H\ ^{12}C\ ^{16}O$); and (iii) the principal axis system for the dipolar hyperfine tensor.

The results of vibronic averaging of the isotropic hfcc's for ^1H (in $^1H\ ^{12}C\ ^{16}O$), ^{13}C (in $^1H\ ^{13}C\ ^{16}O$), and ^{17}O (in $^1H\ ^{12}C\ ^{17}O$) in the lowest six $K = 0$ and 1 levels of the X^2A' state and the lowest eight vibronic levels of the A^2A'' electronic state are presented in Table I. While $K = 0$ vibronic levels belong always to a particular electronic state, their $K = 1$ counterparts are generally shared between both electronic species X^2A' and A^2A''. The mixing with the upper electronic species is insignificant in the lowest $K = 1$ levels assigned to the X^2A' state, because they lie well below the barrier to linearity. Therefore, for the electronic ground state X^2A' the averaged values of $K = 0$ and $K = 1$ vibrational levels reflect only the geometry variation of the electronic mean values of the hfcc in question, resulting in a smooth change of the vibronically averaged hfcc's with increasing v_2 quantum number. A similar behavior is found for the $K = 0$ vibronic levels of the electronically excited state A^2A''. In addition to the geometrical dependence of the electronic hfcc's the vibronically averaged hfcc's of the

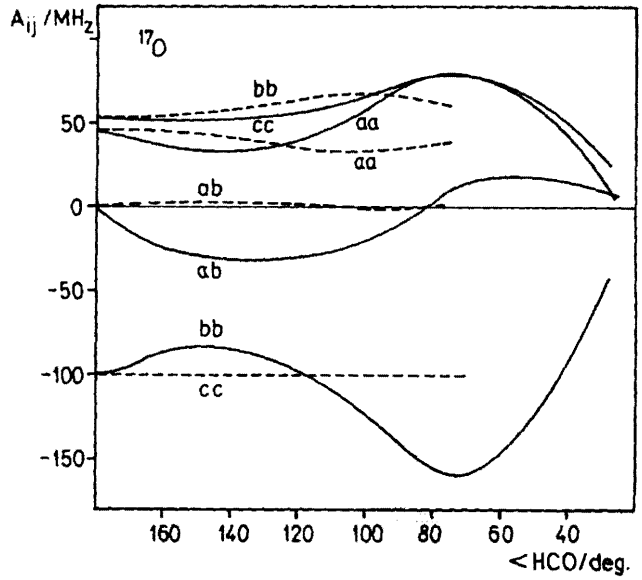

FIG. 12. Angular dependence of the anisotropic hfcc's of ^{17}O. See legend to Fig. 10 for notation.

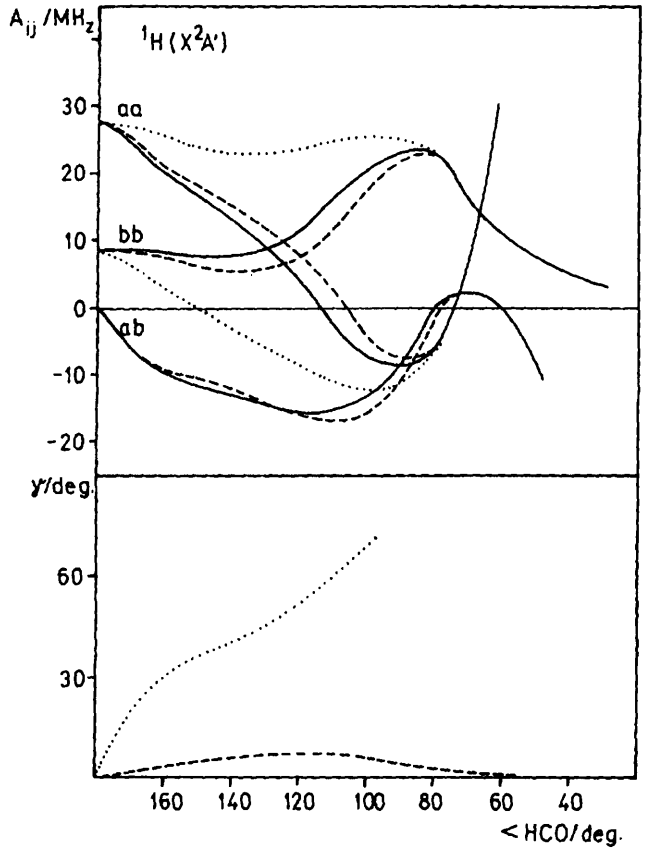

FIG. 13. (Top) Computed bond angle dependence of the components of the anisotropic hf tensor for the hydrogen atom in the X^2A' electronic state at HCO (H–C = 2.127, C–O = 2.221 Bohr) along the axes of the three coordinate systems most frequently employed in experimental and theoretical studies. Full lines are the principal axis system of the electronic spin g tensor (a axis parallel to the C–O bond), dashed lines are the principal moment of inertia axis system (for ^{1}H ^{12}C ^{16}O), and dotted lines are the principal axis system of the dipolar hf tensor. (Bottom) Bond angle dependence of the angle γ between the C–O bond and (i) the z axis of the principal moment of inertia system (dashed line) and (ii) the principal z axis of the hf dipolar tensor (dotted line).

$K = 1$ levels of A^2A'' are also influenced by the mixing between both electronic states because the interaction between both electronic species is strongest in the energy range around the point where they touch each other at the linear geometry. The strong mixing leads to significant irregularities in the dependence of the vibronic hfcc's on the bending quantum number and generally to different values for the vibronic hfcc's of the close lying $K = 0$ and $K = 1$ states above the barrier to linearity. For a more detailed discussion of these effects the reader is referred to Refs. (*28–30*).

4. COMPARISON WITH EXPERIMENTAL FINDINGS AND PREVIOUS THEORETICAL RESULTS

In order to facilitate the comparison with the corresponding experimental (as well as previous theoretical) findings the results of our computations of the isotropic hfcc's

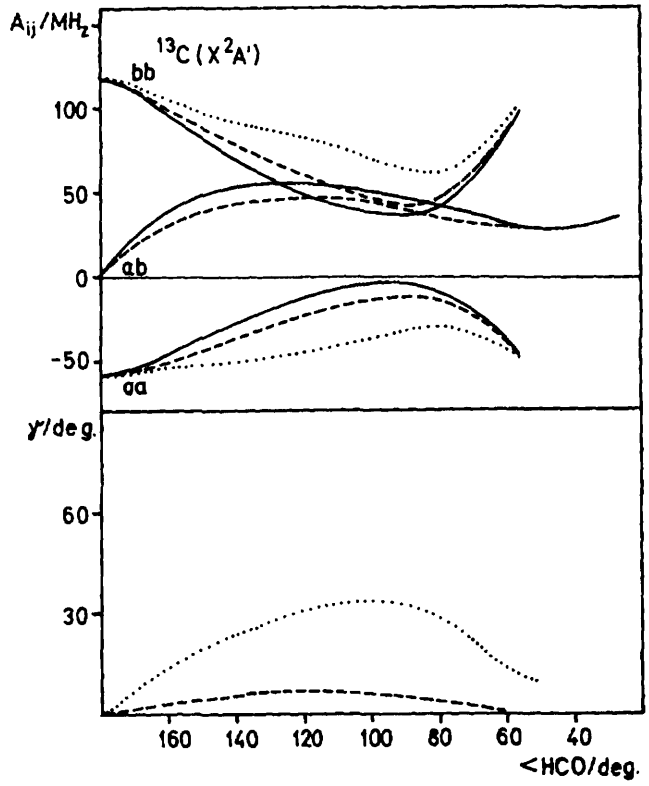

FIG. 14. Bond angle dependence of the anisotropic hfcc's for ^{13}C in different coordinate systems. See legend to Fig. 13 for notation.

in the lowest-lying vibronic level of HCO and DCO ($v_1 = 0$, $v_2 = 0$, $v_3 = 0$, $K = 0$, X^2A' state) are given in Table II. The values for the electronic hfcc's computed at the experimentally derived equilibrium geometry of the X^2A electronic state are also presented to enable a direct comparison with the results of other experimental studies in which vibronic averaging has not been carried out.

An inspection of Table II shows that vibrational/vibronic averaging plays the most important role in the case of the isotropic hfcc for the hydrogen atom. The vibronic mean value for A_{iso} (^1H) differs from its electronic counterpart by 48 or 30 MHz, depending on which set of experimentally derived molecular parameters (*12, 31*) is assumed to represent the equilibrium geometry. Importance of the vibrational averaging was already pointed out by Feller and Davidson (*21*). These authors found that the value they computed at the equilibrium geometry determined by Brown and Ramsay (*29*) should be corrected by 8 MHz due to vibrational averaging effects. In the present study the difference between the vibronic and the electronic isotropic hfcc of the hydrogen center is calculated to be about 20 MHz. We ascribe that to the fact that Feller and Davidson did not carry out an averaging over the bending coordinate and in addition used the harmonic approximation in the description of the stretching modes. From Fig. 4 of the present paper it can be seen, however, that the anharmonicity of the H–C stretching potential curve has nonnegligible effects already for the descrip-

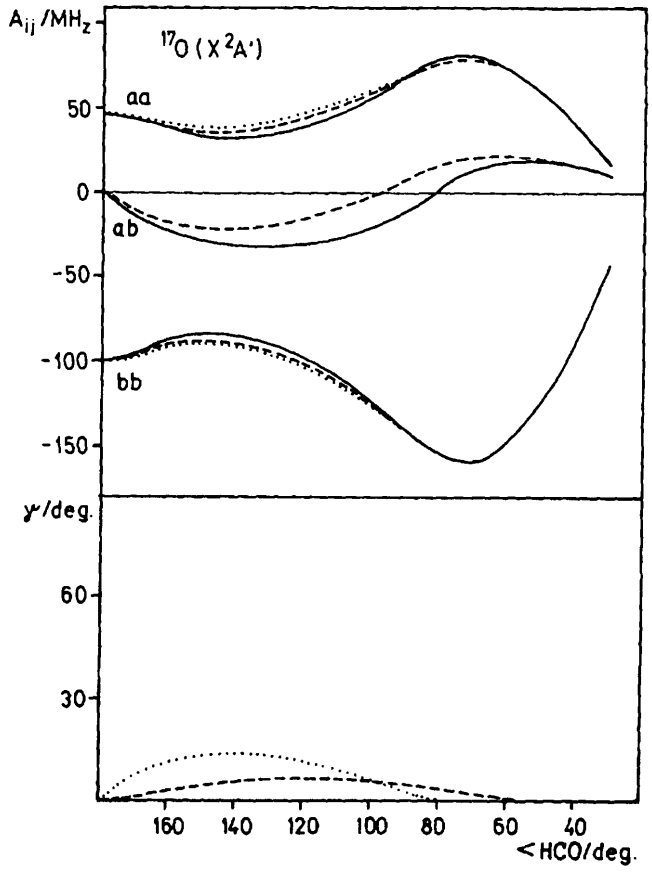

FIG. 15. Angular dependence of the anisotropic hfcc's for ^{17}O in various coordinate systems. See legend to Fig. 13 for notation.

tion of the lowest vibrational state. In combination with the significant nonlinearity of the H–C bond length dependence of the electronic isotropic hfcc for H, a much larger correction of the electronic A_{iso} (^1H) upon vibrational averaging is found.

The results of the present study for the isotropic hfcc's are in very good agreement with available experimental findings. Maximal discrepancies do not exceed 3%. Similar deviations are found between the results of various experimental studies. In the present study the ratio of A_{iso} (^1H) and A_{iso} (D) (obtained from HCO and DCO in its lowest vibrational levels) is calculated to be 6.68. This is in very good agreement with the results of the latest experimental studies (Ref. (*18*) for HCO, Ref. (*17*) for DCO) of 6.65. Both results differ significantly from the ratio of the nuclear g factors of both elements, g_H/g_D, being equal to 6.51. According to the present ab initio investigation the difference in the A_{iso} (^1H)/A_{iso} (^1D) and g_H/g_D ratio is caused predominantly by the above discussed characteristics of the H–C stretching mode; the anharmonicity of the corresponding potential curve and the nonlinearity of the H–C dependence of the hydrogen isotropic hfcc have an appreciately smaller effect on the vibronic mean value of this quantity in the lowest vibronic state of DCO than that in its HCO counterpart.

TABLE I

Results of Computations of the Vibronically Averaged Isotropic hfcc's in the Low-Lying Vibronic Levels of the X^2A' and A^2A'' Electronic States of HCO

atom isotop.	state	K=0			K=1		
		v_2	E (cm^{-1})	A_{iso} (MHz)	v_2	E (cm^{-1})	A_{iso} MHz
H ($H^{12}C^{16}O$)	X^2A'	0	0	383	0	29	384
		1	1094	374	1	1128	375
		2	2175	370	2	2212	371
		3	3246	366	3	3287	367
		4	4306	361	4	4352	362
		5	5356	352	5	5410	354
	A^2A''	0(1)	10103	-89.1	0(2)	10758	-30.5
		1(3)	11686	-89.9	1(4)	12504	103
		2(5)	13245	-90.5	2(6)	13976	-64.6
		3(7)	14768	-90.8	3(8)	15470	-59.8
		4(9)	16258	-90.8	4(10)	16971	-77.7
		5(11)	17731	-90.7	5(12)	18440	-81.6
		6(13)	19208	-90.4	6(14)	19924	-77.4
		7(15)	20703	-90.1	7(16)	21427	-65.7
^{13}C ($H^{13}C^{16}O$)	X^2A'	0	0	388	0	28	388
		1	1088	374	1	1121	374
		2	2163	362	2	2199	362
		3	3227	349	3	3268	349
		4	4281	335	4	4327	336
		5	5326	321	5	5379	322
	A^2A''	0(1)	10092	70.9	0(2)	10734	105
		1(3)	11664	74.9	1(4)	12452	147
		2(5)	13211	79.4	2(6)	13934	91.9
		3(7)	14724	84.5	3(8)	15419	99.0
		4(9)	16204	89.8	4(10)	16911	96.5
		5(11)	17668	94.8	5(12)	18371	101
		6(13)	19134	99.1	6(14)	19843	107
		7(15)	20619	103	7(16)	21332	119
^{17}O ($H^{12}C^{17}O$)	X^2A'	0	0	-41.0	0	29	-40.9
		1	1093	-42.8	1	1126	-42.7
		2	2172	-43.1	2	2209	-43.1
		3	3241	-42.5	3	3281	-42.4
		4	4299	-41.2	4	4346	-41.2
		5	5348	-39.8	5	5401	-39.7
	A^2A''	0(1)	10102	-33.8	0(2)	10754	-34.3
		1(3)	11684	-32.9	1(4)	12492	-36.4
		2(5)	13241	-32.0	2(6)	13969	-32.7
		3(7)	14762	-31.0	3(8)	15461	-35.3
		4(9)	16249	-30.0	4(10)	16961	-31.2
		5(11)	17720	-29.0	5(12)	18428	-29.6
		6(13)	19195	-28.1	6(14)	19908	-29.3
		7(15)	20687	-27.4	7(16)	21408	-30.3

Note. The levels of the upper electronic states are labeled by both "bent" ($v_2 = 0, 1, 2 \ldots$) and "linear" notation ($\nu_2^{lin} = 2\nu_2^{bent} + K + \Lambda$).

Experimental information about the elements of the hf tensor is given in various coordinate systems depending on the experimental technique. From the solid state experiments the components of the hf tensor along the principal axis of the g tensor

TABLE II

Comparison of the Results of the Present Study for Isotropic hfcc's in the Lowest-Lying Vibronic Level ($v_1 = 0$, $v_2 = 0$, $v_3 = 0$) $K = 0$ of the X^2A' Electronic State of HCO with the Corresponding Experimental Findings and the Results of Previous Theoretical Works

atom	this work		exp.		theor.
	elec. averag.	vib. averag.			
H	335[a]	383	383.9[c]	354[d]	375[m]
	353[b]		372.2(4)[e]	389.7(13)[f]	336[n]
			388.9(2)[g]	388.89(12)[h]	329[o]
			388.408(72)[i]		
^{13}C	385[a]	388	377.5[j]	365[d]	562[m]
	398[b]				381[n]
^{17}O	-41.4[a]	-41.0			-18.0[m]
	-41.1[b]				-33.6[n]
D	51.5[a]	57.3	58.0[c]	58.7(2)[g]	
	54.2[b]		60(5)[k]	58.413(74)[l]	

Note. The first set of the values of the present work represents the electronic hfcc's computed at the bond angle value of 125° and the experimentally determined equilibrium bond lengths. The second set is obtained by vibrational averaging assuming that the atoms in question belong to the following isotopomers: H($H^{12}C^{16}O$), C($H^{13}C^{17}O$), O($H^{12}C^{17}O$), and D($D^{12}C^{16}O$). All values are given in MHz. The results correspond to the best energy computed.

[a]H–C = 2.098, C–O = 2.21315 Bohr (*12*).

[b]H–C = 2.127, C–O = 2.221 Bohr (*31*).

[c]Ref. (*5*). [d]Ref. (*7*). [e]Ref. (*9*). [f]Ref. (*13*). [g]Ref. (*15*). [h]Ref. (*16*). [i]Ref. (*18*). [j]Ref. (*6*). [k]Ref. (*11*). [l]Ref. (*17*). [m]Ref. (*19*). [n]Ref. (*21*). [o]Ref. (*30*).

are normally extracted (see, for example, Ref. (*5*)). In experiments performed in gas phase, generally the hf tensor elements along the principal axis of the moment of inertia are given. In many theoretical studies the hf tensor is diagonalized, leading to a third coordinate system, the principal axis system of the hf tensor itself. If all tensor elements are known the transformation between the various axis systems can be performed (*7*). However, because the experimental determination of the outer diagonal elements of the hf tensor is difficult (see Ref. (*32*) for a description) the transformation from one coordinate system into another is often ambiguous because it is not possible to determine exactly the relative orientation of the axis of these coordinate systems. Further difficulties arise because the sign of the hfcc's cannot be determined on the basis of experimental measurements alone. For an analysis of the problems in connection with the HCO radical the reader is referred to Ref. (*19*). It should be kept in mind that isotropic hfcc's and for planar molecules the value of the out of plane component of the anisotropic hf tensor is not affected by the choice of the coordinate system.

To be able to compare the present findings with previous experimental and theoretical results Table III contains the vibronically averaged elements of dipolar hf tensor in all three coordinate systems mentioned above. The different geometrical dependences can be taken from Figs. 13–15.

Let us first focus on the hydrogen values for which most experimental and theoretical data are available. The results computed in the present study are in good agreement (deviation between 0–2 MHz) with recent theoretical works of Davidson and Feller (*21*) and Momose *et al.* (*22*). Also, in comparison to the most recent experimental

TABLE III

Comparison of the Results of the Present Work for Components of the Anisotropic hf Tensor (Electronic Mean Values Computed at the Equilibrium Geometry of the X^2A' State, H–C = 2.098 Bohr, C–O = 2.21315 Bohr (*12*), ⟨HCO = 125°) with the Corresponding Experimental Data and the Results of Previous Theoretical Studies

atom	A_{ij}	C-O=z		phfta			pia				
		this work	exp.	this work	exp.	theor.	this work	exp.			theor.
H	aa	6.33	±14.0[a]	23.4	25[b]	24.9[c]	9.72	10.2[d]	15.2[e]	4.4[f]	3.50[j]
								11.6(2)[g]	11.19[h]	11.23[i]	9.6[m]
	bb	9.73	∓2.2[a]	-7.31	-8[b]	-7.57[c]	6.34	1.6[d]	1.4[e]		11.50[j]
								3.8(2)[g]	2.57(13)[h]	3.14[i]	5.5[m]
	ab	-15.3	16.2[a]	0.0	0.0	0.0	-15.3				-12.0[j]
	cc	-16.1	∓11.8[a]	-16.1	-17[b]	-17.4[c]	-16.1	-11.8[d]	-16.7[e]		-15.0[j]
								-15.5(2)[g]	-13.76(13)[h]	-14.3[i]	-13.6[m]
^{13}C	aa	-16.3		-46.9	-48[b]	-47.4[c]	-27.1				
	bb	53.6		84.3	72[b]	89.7[c]	64.5				
	ab	55.5		0.0	0.0	0.0	47.0				
	cc	-37.4		-37.4	-24[b]	-42.6[c]	-37.4				
^{17}O	aa	37.1		44.2		40.9[c]	42.3				
	bb	-92.4		-99.5		-88.6[c]	-97.6				
	ab	-31.1		0.0		0.0	-16.3				
	cc	55.3		55.3		47.6[c]	55.3				
D	aa	0.972	±2.7[a]	3.59			1.87	1.4(4)[l]		2.191(93)[k]	
	bb	1.49	∓0.3[a]	-1.12			0.598		0.82(80)[l]	0.156(118)[k]	
	ab	-2.34	∓2.4[a]	0.0			-2.27				
	cc	-2.47		-2.47			-2.47		-2.22(80)[l]		

Note. The results are given for the three coordinate systems most frequently used in the literature: (i) the g-tensor principal axis system with the z axis along the C–O bond length (C–O ≡ z); (ii) the system of the principal axis of the anisotropic hf tensor (phfta); and (iii) the principal inertia axis system (pia). All values are given in MHz.

[a]Ref. (*5*). [a*]Ref. (*5*), absolute value. [b]Ref. (*7*). [c]Ref. (*21*). [d]Ref. (*5*), recalculated to pia system in (*15*). [e]Ref. (*7*), recalculated to pia system in (*15*). [f]Ref. (*9*). [f*]Ref. (*9*), assumed value. [g]Ref. (*15*). [h]Ref. (*16*). [i]Ref. (*18*). [j]Ref. (*15*). [k]Ref. (*17*). [l]Ref. (*11*). [m]Ref. (*30*).

investigations (*15, 16, 18*) only small discrepancies are found. Larger relative deviations are obtained for A_{bb} (^{1}H), but the corresponding values are extremely small (≤3 MHz), and large experimental uncertainties have to be taken into account. The values obtained in the pioneering experimental study of Adrian *et al.* (*5*) deviates significantly from other experimental and theoretical studies.

Only one experimental study exists for the anisotropic hfcc of the carbon center (*7*). While only small deviations are found for A_{aa}, larger differences can be seen for A_{bb} and A_{cc}. However, because the values computed in the present study are in good agreement with those obtained in a previous theoretical study of Feller and Davidson, more sophisticated measurements are desirable to clarify the situation. The value of A_{cc} given by Holmberg (*7*) especially lies outside the theoretical error bars.

5. CONCLUSION

To our knowledge this work represents the first ab initio study of the hyperfine structure of the X^2A' and A^2A'' ($1^2\Pi$) system of the formyl radical in which the coupling effects between the electronic states are taken into account. The agreement between the results of the present computations and the corresponding experimental findings is very satisfactory in most instances. For the anisotropic hfcc of the carbon

center larger deviations are found, but because the values obtained in the present work are nearly identical to those computed by Feller and Davidson (*21*) new experimental measurements are desirable. While the experimental data (with few exceptions) are available only for the lowest vibronic level of the X^2A' state, the present study gives the values for hfcc's in all bending states of spectroscopical relevance. We hope that these results will be of interest for experimentalists working on the HCO/DCO system.

ACKNOWLEDGMENT

Financial support by the Deutsche Forschungsgemeinschaft (DFG) in the framework of the Sonderforschungsbereich (SFB) 334 is gratefully acknowledged.

RECEIVED: April 5, 1994

REFERENCES

1. M. PERIĆ, C. M. MARIAN, AND S. D. PEYERIMHOFF, *J. Mol. Spectrosc.* **166**, 000–000 (1994).
2. H. LORENZEN-SCHMIDT, M. PERIĆ, AND S. D. PEYERIMHOFF, *J. Chem. Phys.* **98**, 525–533 (1993).
3. M. PERIĆ AND S. D. PEYERIMHOFF, *J. Mol. Struct.* **297**, 347–359 (1993).
4. M. PERIĆ AND S. D. PEYERIMHFOFF, *J. Chem. Phys.* **98**, 3587–3591 (1993).
5. F. J. ADRIAN, E. L. COCHRAN, AND V. A. BOWERS, *J. Chem. Phys.* **36**, 1661–1672 (1962).
6. E. L. COCHRAN, F. J. ADRIAN, AND V. A. BOWERS, *J. Chem. Phys.* **44**, 4626–4629 (1966).
7. R. W. HOLMBERG, *J. Chem. Phys.* **51**, 3255–3260 (1969).
8. I. C. BOWATER, J. M. BROWN, AND A. CARRINGTON, *J. Chem. Phys.* **54**, 4957–4958 (1971).
9. S. SAITO, *Astrophys. J.* **178**, L95–96 (1972).
10. I. C. BOWATER, J. M. BROWN, AND C. A. CARRINGTON, *Proc. R. Soc. London A* **333**, 265–288 (1973).
11. P. S. H. BOLMAN, J. M. BROWN, A. CARRINGTON, AND G. J. LYCETT, *Proc. R. Soc. London A* **335**, 113–126 (1973).
12. J. A. AUSTIN, D. H. LEVY, C. A. GOTTLIEB, AND H. E. RADFORD, *J. Chem. Phys.* **60**, 207–215 (1974).
13. J. M. COOK, K. M. EVENSON, C. J. HOWARD, AND R. F. CURL, JR., *J. Chem. Phys.* **64**, 1381–1388 (1976).
14. J. W. C. JOHNS, A. R. W. MCKELLAR, AND M. RIGGIN, *J. Chem. Phys.* **67**, 2427–2435 (1977).
15. B. J. BOLAND, J. M. BROWN, AND A. CARRINGTON, *Mol. Phys.* **34**, 453–464 (1977).
16. G. A. BLAKE, K. V. L. N. SASTRY, AND F. C. DELUCIA, *J. Chem. Phys.* **80**, 95–101 (1984).
17. Y. ENDO AND E. HIROTA, *J. Mol. Spectrosc.* **127**, 540–545 (1988).
18. J. M. BROWN, H. E. RADFORD, AND T. J. SEARS, *J. Mol. Spectrosc.* **148**, 20–37 (1991).
19. A. HINCLIFFE AND D. B. COOK, *Chem. Phys. Lett.* **1**, 217–218 (1967).
20. D. C. MCCAIN AND W. E. PALKE, *J. Chem. Phys.* **56**, 4957–4965 (1972).
21. D. FELLER AND E. R. DAVIDSON, *J. Chem. Phys.* **80**, 1006–1017 (1984).
22. T. MOMOSE, M. YAMAGUCHI, AND T. SHIDE, *J. Chem. Phys.* **93**, 7284–7292 (1990).
23. D. CHIPMAN, *Theor. Chim. Acta* **76**, 73–84 (1989).
24. T. H. DUNNING, *J. Chem. Phys.* **90**, 1007–1023 (1989).
25. F. B. VAN DUIJNEVELDT, IBM Research Lab, San Jose, unpublished results, 1971.
26. R. J. BUENKER AND S. D. PEYERIMHOFF, *Theor. Chim. Acta* **35**, 33–58 (1974); **39**, 217–228 (1975); R. J. BUENKER, S. D. PEYERIMHOFF, AND W. BUTSCHER, *Mol. Phys.* **35**, 771–791 (1978); R. J. BUENKER AND R. A. PHILLIPS, *J. Mol. Struct.* **123**, 291–300 (1985); R. J. BUENKER, *Int. J. Quantum Chem.* **29**, 435–460 (1986).
27. B. ENGELS, *Chem. Phys. Lett.* **179**, 398–404 (1991); B. ENGELS, *J. Chem. Phys.* **100**, 1380–1386 (1994).
28. B. ENGELS, M. PERIĆ, W. REUTER, S. D. PEYERIMHOFF, AND F. GREIN, *J. Chem. Phys.* **96**, 4526–4535 (1992).
29. M. PERIĆ AND B. ENGELS, *J. Chem. Phys.* **97**, 4996–5006 (1992).
30. M. PERIĆ, B. ENGELS, AND S. D. PEYERIMHOFF, *in* "Understanding Chemical Reactivity," Vol. 00, "Quantum Mechanical Electronic Structure Calculations with Chemical Accuracy" (S. R. Langhoff, Ed.), Kluwer Academic, Dordrecht, The Netherlands, in press.
31. J. M. BROWN AND D. A. RAMSAY, *Can. J. Phys.* **53**, 2232–2241 (1975).
32. T. J. SEARS, *Comp. Phys. Rep.* **2**, 1–32 (1984).